

A Constraint Relationship for Reflectional Symmetry and Rotational Symmetry

Dinggang Shen¹, Horace H. S. Ip² and Eam Khwang Teoh³

¹ Department of Radiology, Johns Hopkins University
Email: dgshen@cbmv.jhu.edu

² Department of Computer Science, City University of Hong Kong, Hong Kong
Email: cship@cityu.edu.hk

³ School of Electrical and Electronic Engineering, Nanyang Technological University, Singapore
Email: eekteoh@ntu.edu.sg

Abstract

A novel theorem linking reflectional symmetry and rotational symmetry has been established in this paper. This theorem constrains that, for a rotationally symmetric image with $K \geq 1$ fold(s) (K -RSI), its number of reflection-symmetric axes must be either K or zero. The novel constraint theorem provides the guidance for the procedure of symmetry detection. It has been demonstrated by the experiments included in this paper.

Key words – symmetry detection, symmetric axis, reflectional axes, rotationally symmetric image

1. Introduction

Rotational symmetry and reflectional symmetry have been studied extensively in the areas of computer vision [13,14]. Many techniques have been suggested for detecting either reflection-symmetric axes [1-3] or rotationally symmetric axes [4-7] of planar images. Furthermore, techniques able to detect both reflectional symmetry and rotational symmetry [8-9] have also been reported. However, to the author's knowledge, none of the previous papers in the computer vision area studied the relationship between reflectional symmetry and rotational symmetry.

Here, we investigate this relationship by studying the definitions and the properties associated with both reflectional symmetry and rotational symmetry. The result is, *for any planar image the number of reflection-symmetric axes is either K or zero for a K -RSI, where $K \geq 1$.*

2. Properties on reflectional and rotational symmetries

2.1 Reflectional symmetry

A planar image is said to be reflection-symmetric if it is invariant to reflection(s) with respect to one or more straight lines, denoted as *reflection-symmetric axes*. Notice that the concept of mirror symmetry is usually utilized for an object with only *one* reflection-symmetric axis. The reflection-symmetric axes can be proved to pass through the center of mass of the image. In the following, for ease of discussion and without loss of generality, we assume that every image has been centered at its geometric center. Then, the reflection-symmetric image should satisfy: $f(r, \mathbf{f} + \mathbf{q}) = f(r, \mathbf{f} - \mathbf{q})$, where \mathbf{f} is the angle of the reflection-symmetric axis.

Without loss of generality, let's assume that the studied image has maximum $M > 0$ reflection-symmetric axes and the angles of these reflection-symmetric axes are respectively

$$0 = \mathbf{y}_0 < \mathbf{y}_1 < \mathbf{y}_2 < \dots < \mathbf{y}_{M-1} < \mathbf{p}.$$

Then we can obtain the following theorem that describes the relationship between the angles of the reflection-symmetric axes.

Theorem 2.1 The angle difference between any pair of reflection-symmetric axes is a multiple of $\frac{\mathbf{p}}{M}$. That is, $\mathbf{y}_{i+1} - \mathbf{y}_i = \frac{\mathbf{p}}{M}$, for $i = 0, 1, \dots, M - 2$.

Proof:

We have assumed that $0 = \mathbf{y}_0 < \mathbf{y}_1 < \mathbf{y}_2 < \dots < \mathbf{y}_{M-1} < \mathbf{p}$. Accordingly, from the reflectional axis with angle $\mathbf{y}_0 = 0$, we have

$$f(r, \mathbf{q}) = f(r, -\mathbf{q}). \quad (1)$$

Also from the reflectional axis with angle \mathbf{y}_1 , we have

$$f(r, \mathbf{q} + \mathbf{y}_1) = f(r, \mathbf{y}_1 - \mathbf{q}). \quad (2)$$

Based on the two above-mentioned equations, we can obtain $f(r, \mathbf{q} + 2\mathbf{y}_1) = f(r, 2\mathbf{y}_1 - \mathbf{q})$ by the following steps.

$$f(r, \mathbf{q} + 2\mathbf{y}_1) = f(r, (\mathbf{q} + \mathbf{y}_1) + \mathbf{y}_1) = f(r, \mathbf{y}_1 - (\mathbf{q} + \mathbf{y}_1)) = f(r, -\mathbf{q}) = f(r, \mathbf{q}),$$

$$f(r, 2\mathbf{y}_1 - \mathbf{q}) = f(r, \mathbf{y}_1 - (\mathbf{q} - \mathbf{y}_1)) = f(r, (\mathbf{q} - \mathbf{y}_1) + \mathbf{y}_1) = f(r, \mathbf{q}).$$

Similarly, we can obtain $f(r, \mathbf{q} + n\mathbf{y}_1) = f(r, n\mathbf{y}_1 - \mathbf{q})$ for $n \geq 3$, by using equations (3) and (4):

$$f(r, (n-2)\mathbf{y}_1 - \mathbf{q}) = f(r, \mathbf{q} + (n-2)\mathbf{y}_1) \quad (3)$$

$$f(r, (n-1)\mathbf{y}_1 - \mathbf{q}) = f(r, \mathbf{q} + (n-1)\mathbf{y}_1). \quad (4)$$

The following steps give the process of obtaining this result.

$$\begin{aligned} f(r, \mathbf{q} + n\mathbf{y}_1) &= f(r, (\mathbf{q} + \mathbf{y}_1) + (n-1)\mathbf{y}_1) = f(r, (n-1)\mathbf{y}_1 - (\mathbf{q} + \mathbf{y}_1)) = f(r, (n-2)\mathbf{y}_1 - \mathbf{q}) \\ &= f(r, (n-2)\mathbf{y}_1 + \mathbf{q}), \\ f(r, n\mathbf{y}_1 - \mathbf{q}) &= f(r, (n-1)\mathbf{y}_1 - (\mathbf{q} - \mathbf{y}_1)) = f(r, (\mathbf{q} - \mathbf{y}_1) + (n-1)\mathbf{y}_1) = f(r, \mathbf{q} + (n-2)\mathbf{y}_1). \end{aligned}$$

In this way, we know the axes with angles $\{\mathbf{y}_0 = 0, \mathbf{y}_1, 2\mathbf{y}_1, 3\mathbf{y}_1, \dots, n\mathbf{y}_1, \dots\}$ are also reflection-symmetric axes. Comparing two angle sets $\{\mathbf{y}_0 = 0, \mathbf{y}_1, 2\mathbf{y}_1, 3\mathbf{y}_1, \dots, n\mathbf{y}_1, \dots\}$ and $\{0 = \mathbf{y}_0 < \mathbf{y}_1 < \mathbf{y}_2 < \dots < \mathbf{y}_{M-1} < \mathbf{p}\}$, it is easy to conclude that \mathbf{y}_i should satisfy the requirements $\mathbf{y}_i = (i-1)\mathbf{y}_1$ for $i = 2, 3, \dots, M-1$ and $\mathbf{y}_i = i\frac{\mathbf{p}}{M}$ for $i = 1, 2, \dots, (M-1)$. Accordingly, the angle difference between any pair of reflection-symmetric axes is a multiple of $\frac{\mathbf{p}}{M}$. #

2.2 Rotational symmetry

A planar image is said to be order K rotationally symmetric, if it is invariant under rotation of $2\mathbf{p}/K$ radians about the center of mass of the object and K is the largest integer. This planar image is usually called a rotationally symmetric image with K folds (K -RSI). The orientations of these K folds can be defined by K fold axes.

The mathematical definition of a K -RSI, $f(r, \mathbf{q})$, can be described as

$$f(r, \mathbf{q}) = f(r, \mathbf{q} + \frac{(i-1) \times 2\mathbf{p}}{K}), \quad i = 1, 2, \dots; \quad \mathbf{q} \in [0, 2\mathbf{p}).$$

3. A Theorem linking reflectional symmetry and rotational symmetry

Based on the above properties derived respectively for reflectional symmetry and rotational symmetry, this section investigates the relationship (Theorem 3.1) linking the number of the reflection-symmetric axes with the number of the fold axes for any planar image. It can be used as a

means of double checking the correctness of any symmetry detection techniques, and simultaneously as guidance for the symmetry detection procedure.

Theorem 3.1 (1) For a K -RSI ($K \geq 1$), the number of the reflection-symmetric axes is either 0 or K .

(2) On the other hand, if the detected number of the reflection-symmetric axes is not equal to zero, then this number is exactly the fold number.

Proof:

It is easy to prove the case that no any reflection-symmetric axis exists. Accordingly, we only need to prove the case that there do exist some reflection-symmetric axes. Let M be the number of the reflection-symmetric axes, and K be the fold number. In the following, we prove that (a) $M \geq K$ and (b) $K \geq M$, which leads to $M = K$.

(a) For K -RSI ($K \geq 1$), if there exist any reflection-symmetric axes, then the number of the reflection-symmetric axes M must be greater than or equal to the fold number K ($M \geq K$).

If the studied image $f(r, \mathbf{q})$ is not reflection-symmetric, then its number of the reflection-symmetric axes will be zero. Otherwise, if $f(r, \mathbf{q})$ is reflection-symmetric, we can assume that x -axis is its reflection-symmetric axis. That is $f(r, -\mathbf{q}) = f(r, \mathbf{q})$. Since $f(r, \mathbf{q} + \frac{2\mathbf{p}}{K}k) = f(r, \mathbf{q})$ for $k=1, \dots, (K-1)$, then $f(r, -\mathbf{q} + \frac{2\mathbf{p}}{K}k) = f(r, -\mathbf{q})$ for $k=1, \dots, (K-1)$. Using both $f(r, -\mathbf{q}) = f(r, \mathbf{q})$ and $f(r, \mathbf{q} + \frac{2\mathbf{p}}{K}k) = f(r, \mathbf{q})$, we have $f(r, -\mathbf{q} + \frac{2\mathbf{p}}{K}k) = f(r, -\mathbf{q}) = f(r, \mathbf{q}) = f(r, \mathbf{q} + \frac{2\mathbf{p}}{K}k)$. That is, the lines with angles of $\frac{2\mathbf{p}}{K}k$, for $k=1, \dots, (K-1)$, are also the reflection-symmetric axes.

Accordingly, if there exist any reflection-symmetric axes, the number of the reflection-symmetric axes must be greater than or equal to K . That is $M \geq K$.

(b) For the image with $M > 0$ reflection-symmetric axes, its fold number K must be greater than or equal to M ($K \geq M$).

Without lose of generality, let's assume the angles for these reflection-symmetric axes are

$0 = \mathbf{y}_0 < \mathbf{y}_1 < \mathbf{y}_2 < \dots < \mathbf{y}_{M-1} < \mathbf{p}$. From Theorem 2.1, we know $\mathbf{y}_i = i \frac{\mathbf{p}}{M}$ for $i = 1, 2, \dots, (M-1)$.

Using $f(r, \mathbf{q} + \mathbf{y}_1) = f(r, \mathbf{y}_1 - \mathbf{q})$ and $f(r, -\mathbf{q}) = f(r, \mathbf{q})$, we have

$$f(r, \mathbf{q} + 2\mathbf{y}_1) = f(r, (\mathbf{q} + \mathbf{y}_1) + \mathbf{y}_1) = f(r, \mathbf{y}_1 - (\mathbf{q} + \mathbf{y}_1)) = f(r, -\mathbf{q}) = f(r, \mathbf{q}).$$

That is $f(r, \mathbf{q} + 2\mathbf{y}_1) = f(r, \mathbf{q})$. On the other words, the studied image $f(r, \mathbf{q})$ is rotationally

symmetric at an angle $2\mathbf{y}_1$. Since $2\mathbf{y}_1 = 2\frac{\mathbf{p}}{M}$, the number of the *known* fold axes is thus

$2\mathbf{p}/(2\mathbf{y}_1) = M$. That is, the *actual* fold number K must be greater than or equal to M , i.e. $K \geq M$.

The proof in (a) indicates that, for a K -RSI, if there exist any reflection-symmetric axes, the number of the reflection-symmetric axes M must be *greater than or equal to* the fold number K , i.e. $M \geq K$.

While the proof in (b) indicates that, for the image with $M > 0$ reflection-symmetric axes, its fold number K must be *greater than or equal to* M , i.e. $K \geq M$. To satisfy both $M \geq K$ and $K \geq M$, M should be equal to K . That is, $K = M$. Therefore, we have proven that, if there exist any reflection-symmetric axes, the number of reflectional axes should be equal to the fold number.

4. Experimental Results

In the experiments, we provide some examples to show the correctness of the novel constraint theorem on symmetries (Section 4.1), and also demonstrate the helpfulness of the new constraint theorem in the procedure of symmetry detection.

4.1 Demonstration of the correctness of the constraint theorem

Images in figure 1 have different fold numbers, ranging from 1 to 4. Both images in figures 1(a1) and 1(a2) are 1-RSIs, i.e. fold number is 1. Figure 1(a1) is not reflection-symmetric, and then the number of reflection-symmetric axes is zero. While figure 1(a2) is reflection-symmetric, whose number of reflection-symmetric axes is 1, exactly equal to fold number 1. A thin line in figure 1(a2) denotes the reflection-symmetric axis of image. From these two examples, it is easy to infer, for a 1-RSI, the number of reflection-symmetric axes is either 1 or zero.

Two images in figures 1(b1) and 1(b2) are both 2-RSIs. Two fold axes are shown as two arrows. Figure 1(b1) is not reflection-symmetric, that is, the number of reflection-symmetric axes is *zero*. But, figure 1(b2) is reflection-symmetric. Two reflection-symmetric axes are shown as two thin lines in figure 1(b2), where one line is overlapping with the two fold axes. Accordingly, it has been proved that for a 2-RSI the number of reflection-symmetric axes is either 2 or *zero*.

Two images in figures 1(c1) and 1(c2) are 3-RSIs, while the last pair of images in figures 1(d1) and 1(d2) are 4-RSIs. Arrows in the corresponding figures represent the fold axes, and thin lines denote the reflection-symmetric axes. The experimental results on these four images also show, the number of reflection-symmetric axes is either equal to the *fold number* (3 or 4) or *zero*.

The symmetry detection results in Figure 1 were obtained by using a technique suggested in [11], which is based on Generalized Complex moments. Using this technique, we can also check the correctness of the constraint theorem on grey-level images (Figure 2), and even the noise-corrupted images (Figure 3). Paper [11] has shown that its symmetry detection technique is robust to random noises, because of using the global moments. As to the sensitivity of the symmetry detection method to errors in the placement of the origin, please refer to [12], where the proposed symmetry detection method is also based on Generalized Complex moments.

4.2 Demonstration of the usefulness of the constraint theorem in symmetry detection

The novel constraint theorem is also useful for some available methods in their symmetry detection. For example, Sun [5,10] has proposed two different methods to respectively detect reflectional symmetry [10] and rotational symmetry [5], based on the same gradient orientation histogram. In reflectional symmetry detection, he used the convolution of the histogram with itself that produces the peaks at the symmetric angles. In rotational symmetry detection, he used Fourier transformation on the histogram and regarded the fold number as the first order that makes the Fourier coefficient nonzero. Since these techniques use local features, i.e. gradient orientations, for symmetry detection, they are effective and applicable to images with background intensity gradient. But these techniques

fail for certain types of degraded images. The novel constraint theorem can be applied to detecting and correcting for erroneous detection.

For the image with white background in Figure 4, the rotational symmetry detection method in [5] detected three fold axes, although the actual fold number of this image is only one. The reflectional symmetry detection method in [10] detected unique reflectional axis that is indicated as a thin line in Figure 4. Using our novel constraint theorem, it is easy to conclude that at least one of the symmetry detection results is incorrect. After analysis, we can find that two of the three fold axes should be removed. From this example, it is simple to observe that, when different techniques were used to detect reflectional and rotational symmetries, the novel constraint theorem can be used as a helpful tool for guiding symmetry detection process.

5. Conclusion

In this paper, we have presented a theorem that governs the number of the reflection-symmetric axes and the number of the rotational symmetric axes for any planar image. The theorem states that for any K -RSI, its number of reflection-symmetric axes is either zero or K . From other viewpoints, we can say, if the detected number of reflection-symmetric axes is not zero, then this number is exactly the fold number of the image under study.

The theorem can be applied to checking the correctness of the results in the symmetry detection, and also guiding the procedure of symmetry detection.

Acknowledgement:

This work is partially supported by a HKSAR Research Grant Council, CERG grant No. 9040437/CityU 1113/99E.

Reference:

1. T. Zielke, M. Brauckmann and W.V. Seelen, "Intensity and edge-based symmetry detection with an application to car-following", *Computer Vision, Graphics, and Image Processing: Image Understanding*, Vol.58, No.2, pp.177-190, 1993.
2. M. Atallah, "On symmetry detection", *IEEE Trans. on computer*, Vol.34, No.7, 1985.
3. G. Marola, "On the detection of the axes of symmetry of symmetric and almost symmetric planar images", *IEEE Trans. on Pattern Analysis and Machine Intelligence*, Vo.11, No.1, pp.104-108, 1989.
4. S.C. Pei and C.N. Lin, "Normalization of rotationally symmetric shapes for pattern recognition", *Pattern Recognition*, Vol.25, No.9, pp.913-920, 1992.
5. C. Sun, "Fast recovery of rotational symmetry parameters using gradient orientation", *SPIE Journal of Optical Engineering*, Vol.36, No.4, pp.1073-1077, 1997.
6. J.C. Lin, W.H. Tsai, and J.A. Chen, "Detecting number of folds by a simple mathematical property", *Pattern Recognition Letters*, Vol.15, pp.1081-1088, 1994.
7. Dinggang Shen, Horace H.S. Ip, "Generalized affine invariant image normalization", *IEEE Trans. on PAMI*, 19(5):431-440, May 1997.
8. T. Masuda, K. Yamamoto and H. Yamada, "Detection of partial symmetry using correlation with rotated-reflected images", *Pattern Recognition*, Vol.26, No.8, 1993.
9. C. Sun and J. Sherrah, "3D symmetry detection using the extended Guassian image", *IEEE Trans. on Pattern Analysis and Machine Intelligence*, Vol.19, No.2, 1997.
10. C. Sun and D. Si, "Fast reflectional symmetry detection using orientation histograms", *Journal of Real-Time Imaging*, 5(1):63-74, February 1999.
11. Dinggang Shen, Horace H.S. Ip, Kent K.T. Cheung, and E.K. Teoh, "Symmetry detection by generalized complex (GC) moments: a close-form solution", *IEEE Trans. on PAMI*, 21(5):466-476, May 1999.
12. Dinggang Shen, Horace H.S. Ip, and E.K. Teoh, "An energy of asymmetry for accurate detection of global reflection axes", *Image and Vision Computing*, 19(5): 283-297, April 2001.
13. H. Wely, *Symmetry*, Princeton Univ. Press, 1952.
14. W. Miller, *Symmetry Groups and their Application*, Academic Press, 1972.

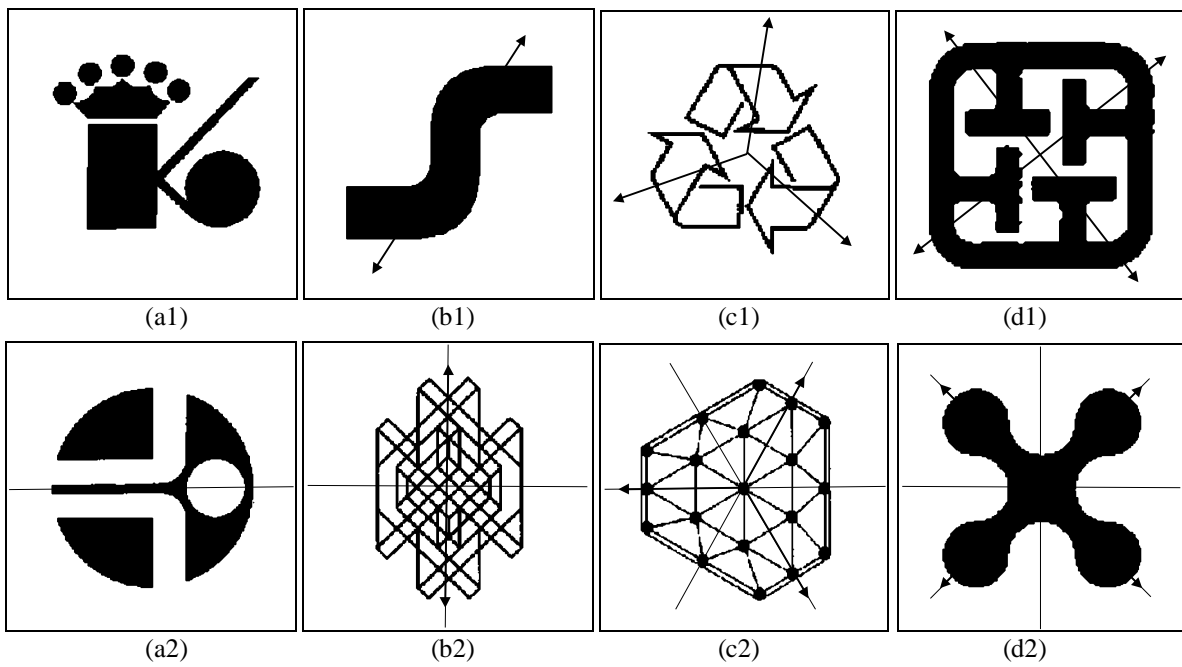


Figure 1 Experimental results showing the relationship between reflectional symmetry and rotational symmetry. Images in (a1-d1) are not reflection-symmetric, that is, the number of reflection-symmetric axes is zero even though these images have different fold numbers, ranging from 1 to 4. Images in (a2-d2) are reflection-symmetric. The numbers of reflection-symmetric axes for these images are respectively equal to the fold numbers of the associated images, i.e. from 1 to 4. Arrows denote the fold axes, while thin lines denote the reflection-symmetric axes.

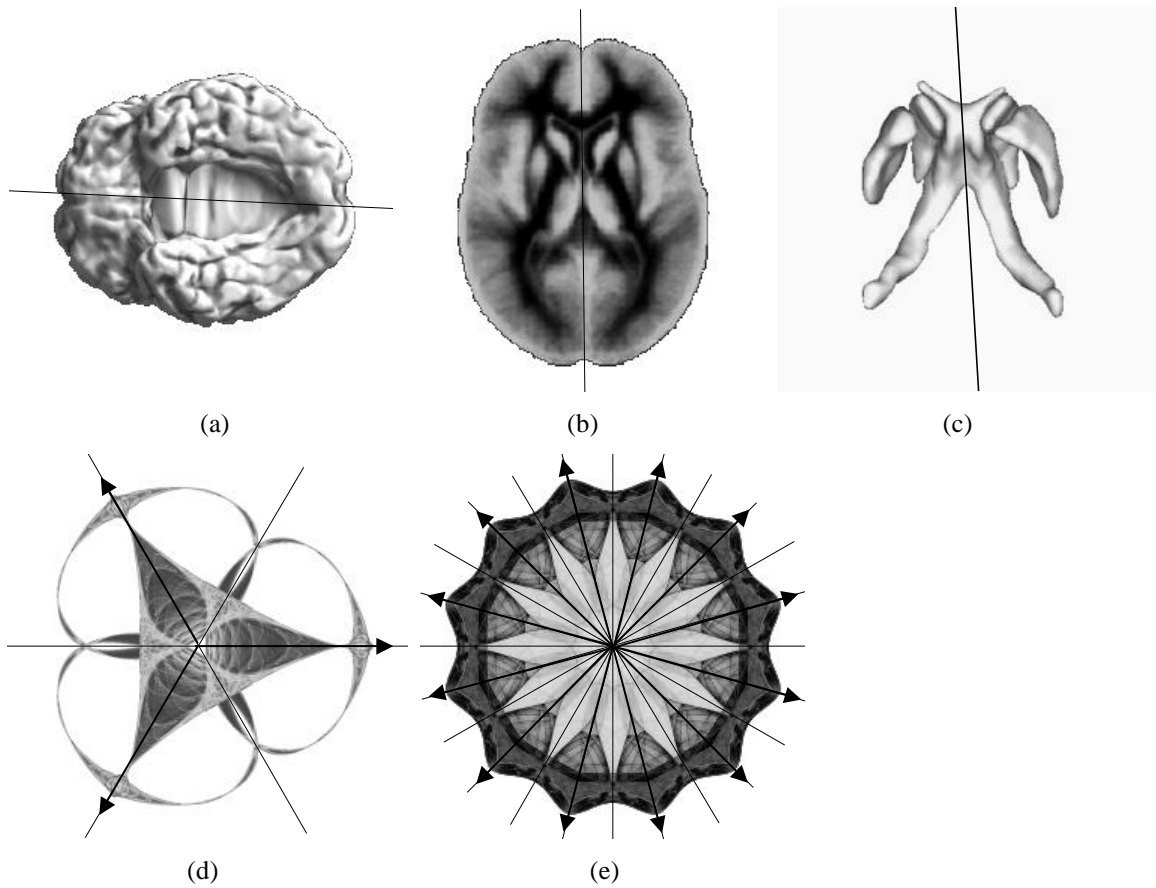


Figure 2 Experimental results on gray-level images showing the relationship between reflectional symmetry and rotational symmetry. (a) Human brain image (fold number 1), (b) a slice of the average brain image (fold number 1), (c) brain ventricle image (fold number 1), (d) image with fold number 3, and (e) image with fold number 12. The lines and arrows have the same meanings as those in Figure 1.

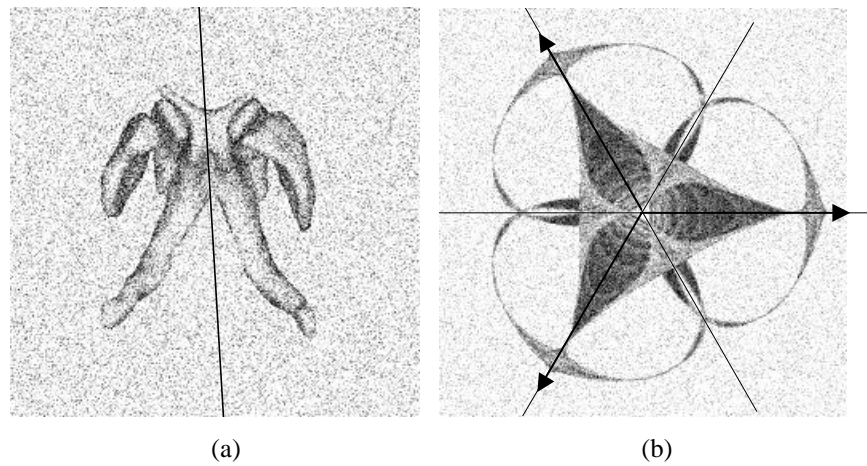


Figure 3 Experimental results on noise-corrupted gray-level images. (a) A brain ventricle image with fold number 1, and (b) an image with fold number 3.

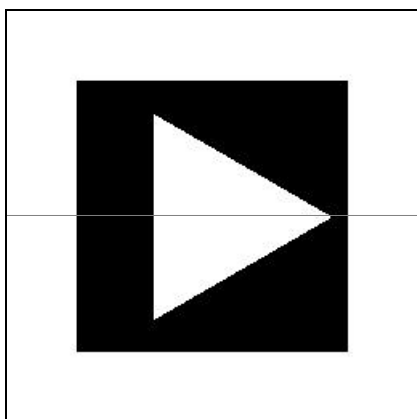


Figure 4 An example demonstrating the effectiveness of using the novel constraint theorem in the procedure of symmetry detection that is based on the different techniques. For example, the rotational symmetry detection method in [5] detected three fold axes, while the reflectional symmetry detection method in [10] detected only one reflectional axis. Using the novel constraint theorem and some analyses, it's easy to infer that the fold number should be one.